Electronic Supplementary Material (ESI) for Physical Chemistry Chemical Physics.

Supporting Information

Slip divergence of water flow in graphene nanochannels: The role of chirality†

Enrique Wagemann[a], Elton Oyarzua[a],Jens H. Walther[b,c],Harvey A. Zambrano*[a]

[a] *Universidad de Concepcion, Concepcion, Chile. Tel: 56 41266 1468; E-mail: harveyzambrano@udec.cl*
[b] *Technical University of Denmark, Copenhagen, Denmark.*
[c] *Chair of Computational Science, ETH Zurich, Zurich, Switzerland.*

Slip length calculations

Slip length (l_s) is calculated following the P5 procedure of Kannam et al.[1]. First the volumetric flow ($Q_{measured}$) is calculated from the mass flow. The mass flow was measured by counting the number of molecules crossing a fixed plane in the streaming direction per unit of time[1,2]. The mass flow is then divided by the measured channel density to obtain the volumetric flow. Then the enhancement is calculated as

$$\varepsilon = Q_{measured}/Q_{H-P}$$

where Q_{H-P} corresponds to the Hagen-Poiseuille solution for a developed laminar flow of a incompressible newtonian fluid under a pressure gradient between two infinite parallel Plates:

$$\frac{Q_{H-P}}{w} = \frac{1}{12\mu}\left[\frac{h^3 \Delta P}{L}\right]$$

where h corresponds to the channel height. This height is calculated as the average distance between the innermost graphene layers, subtracting the Van der Waals size of the carbon atoms (0.34 nm). ΔP is estimated as: $\Delta P = \rho a L$, where a corresponds to acceleration of the applied external field, L is the channel length and ρ is overall channel density. w corresponds to the channel width. The bulk viscocity (μ) for the SPC/E water model is taken from literature[3].

The slip length is finally calculated from ε as

$$l_s = \frac{h(\varepsilon - 1)}{6}$$

Temperature profiles

The fluid temperature profiles for the armchair 2.8 nm cases are presented in Figure 1. For the low forcing cases a constant temperature around 296 K is calculated in the bulk zone (below $4 \cdot 10^{11}$ m/s^2). After divergence is reached (around $6 \cdot 10^{11}$ m/s^2) temperature starts to increase, showing a decrease in the momentum transfer between fluid and wall. The temperature profiles display a non-newtonian behaviour at the interface. When compared to the density profiles the temperature peaks seem to coincide with the depletion layer. Note that the temperature increase affects the whole profile. When normalizing the temperature profiles to the bulk temperature no difference is found between cases, as seen in Figure 2, showing that the temperature increase due to viscous heating is proportional across the channel.

To ensure that the obtained velocity increase isn't related to a viscosity decrease due to the temperature increase, we coupled the thermostat to both graphene and water on high forcing cases were divergence is obtained. A clear difference in the temperature is observed when both are compared (figure 3). When comparing the obtained flow velocity (mean velocity) no major difference is observed, as for the only graphene coupled case a mean velocity of 179 m/s is obtained and for the both water and graphene case a mean velocity of 183 m/s ($\sim$ 2 % difference). The same is observed for other cases with other level of forcing ($8 \cdot 10^{11}$ m/s^2 and $12 \cdot 10^{11}$ m/s^2). When comparing cases on which GE and water are thermostated and the same force is applied but the direction changes (AC vs ZZ) a similar difference between velocity is obtained ($\sim$ 10 % difference between AC an ZZ) when comparing to the cases on which only the graphene is coupled to the thermostat. The temperature profiles of the both GE and Water coupled cases show no difference when compared between AC and ZZ cases and different applied force ($8 \cdot 10^{11}$ m/s^2 and $10 \cdot 10^{11}$ m/s^2.

Figure 4A shows a comparison of the temperature profiles for the AC and ZZ cases when divergence is reached. A difference can be observed, on which the AC temperature is higher than the ZZ case. This can be better appreciated when a zoom is made to the bulk zone (Figure 4B). This temperature difference can be related to a difference in the wall-fluid momentum transfer. A lower momentum transfer between wall-fluid would result in a lower friction and thus greater flow velocities.

Shear rate

Figure 5 shows the calculated shear rate as a function of the shear stress. The shear rate shows a linear dependence to the shear stress, demonstrating that the bulk fluid remains newtonian.

References

[1] S. K. Kannam, B. Todd, J. S. Hansen and P. J. Daivis, *J. Chem. Phys.*, 2012, **136**, 024705.

[2] K. Ritos, D. Mattia, F. Calabrò and J. M. Reese, *J. Chem. Phys.*, 2014, **140**, 014702.

[3] M. A. González and J. L. Abascal, *J. Chem. Phys.*, 2010, **132**, 096101.

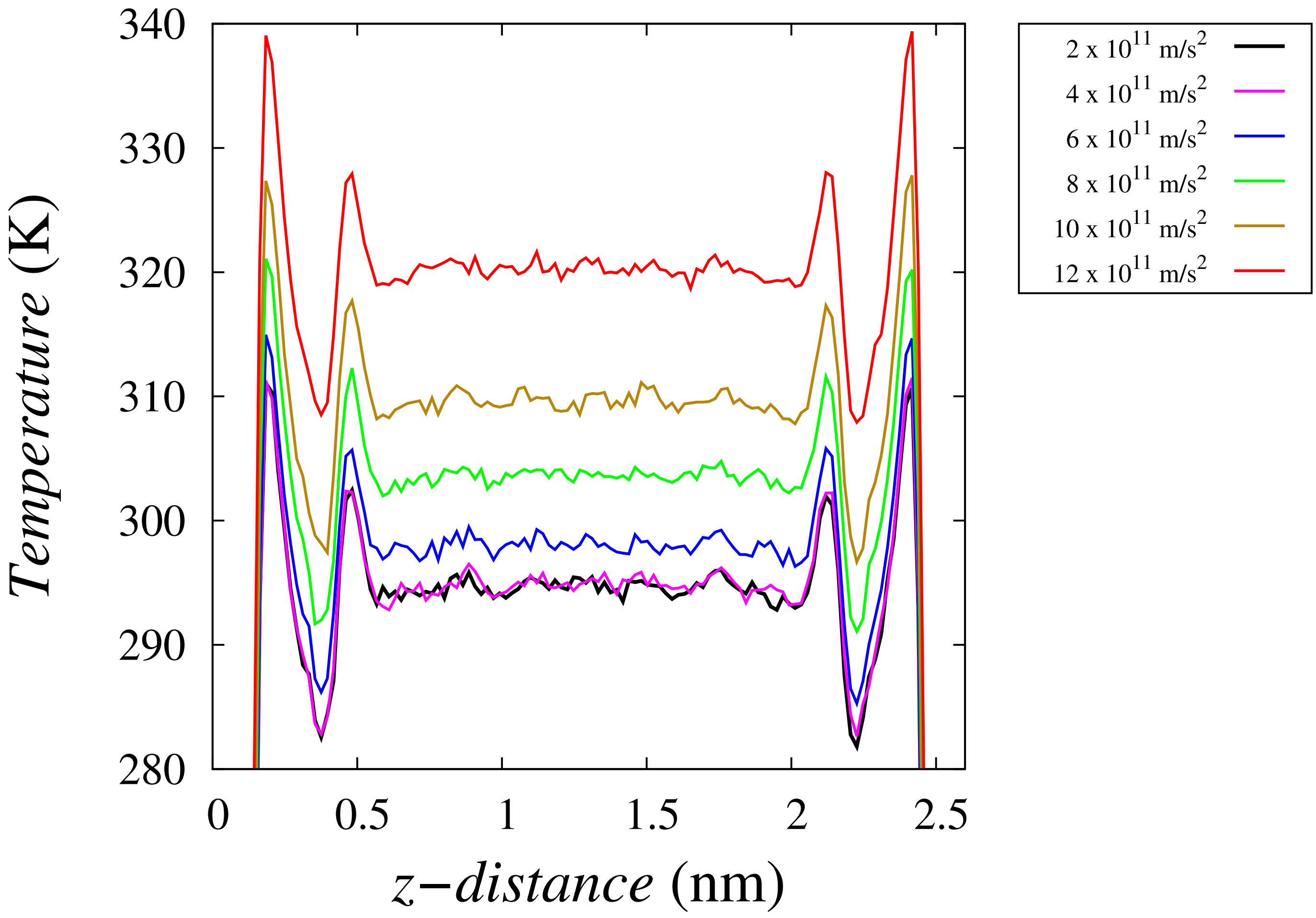

Figure 1 Temperature profiles for the different applied external force for the 2.8 nm armchair case. The wall temperature was maintained constant at 300 K by coupling its atoms to a Berendsen thermostat

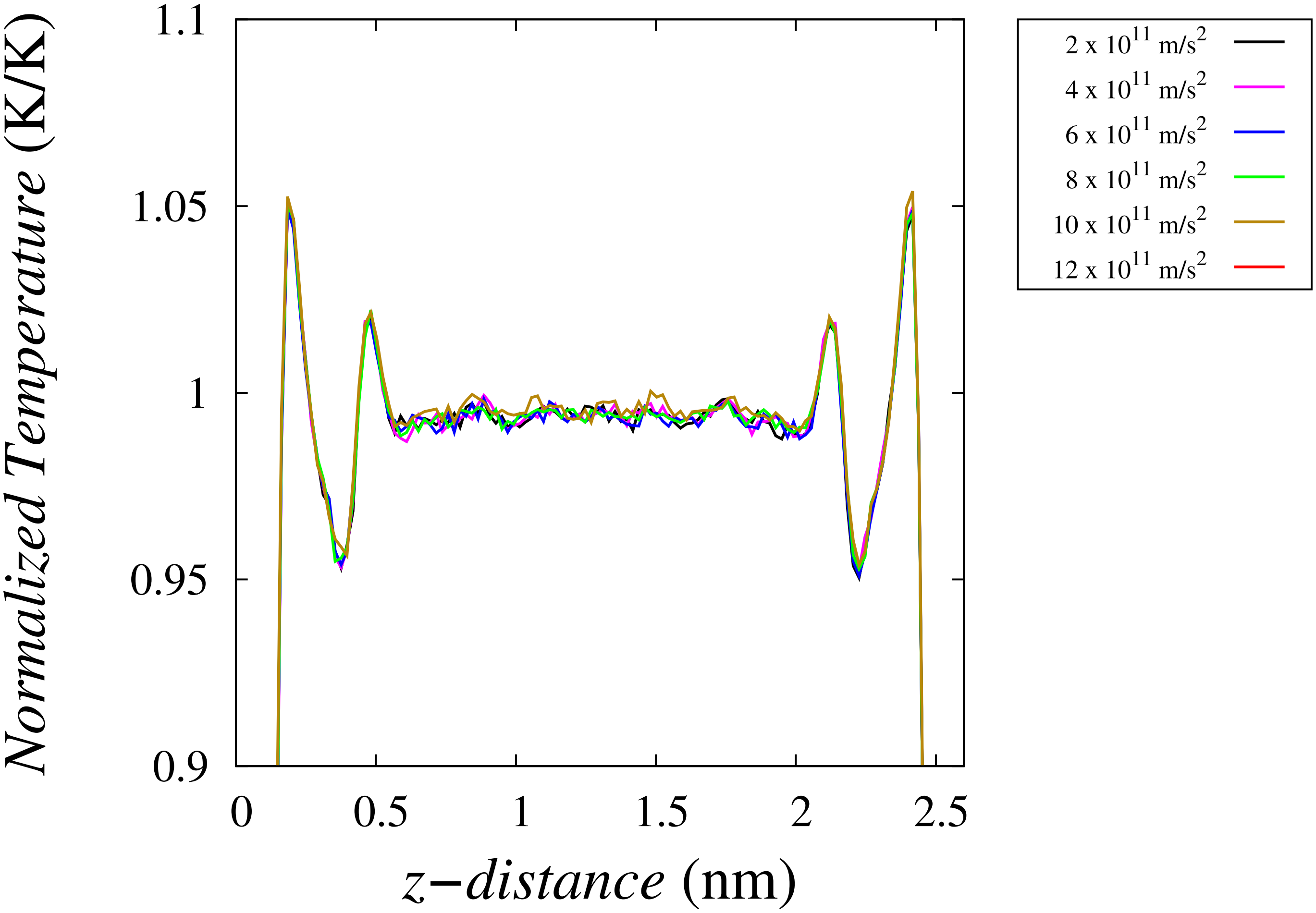

Figure 2 Normalized temperature profiles for the different applied external force for the 2.8 nm armchair case.

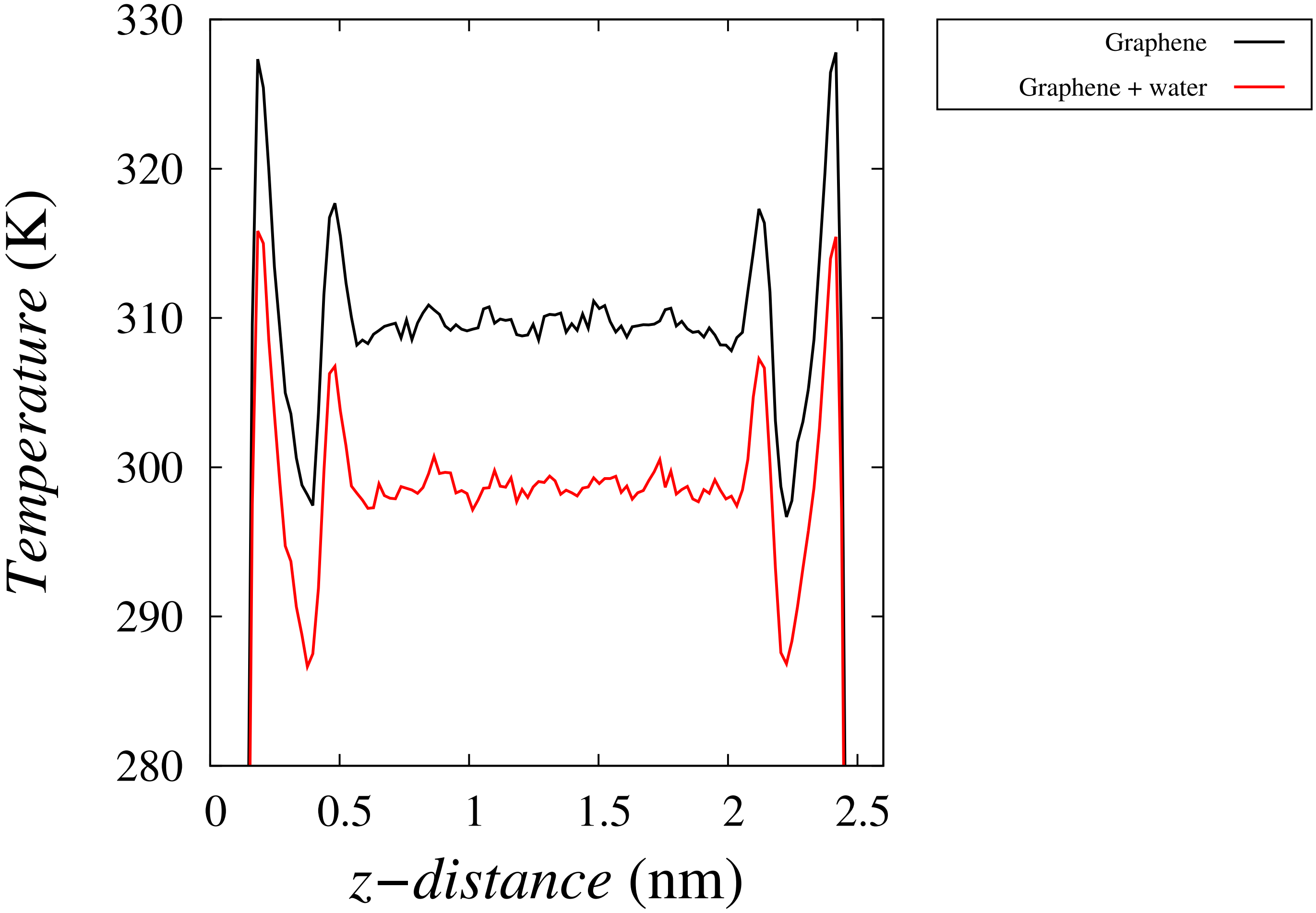

Figure 3 Temperature profiles for the $10 \cdot 10^{11}$ m/s^2 applied external force for the 2.8 nm armchair case. The thermostat was coupled to the graphene atoms (black line) and to graphene atoms and water molecules (red line).

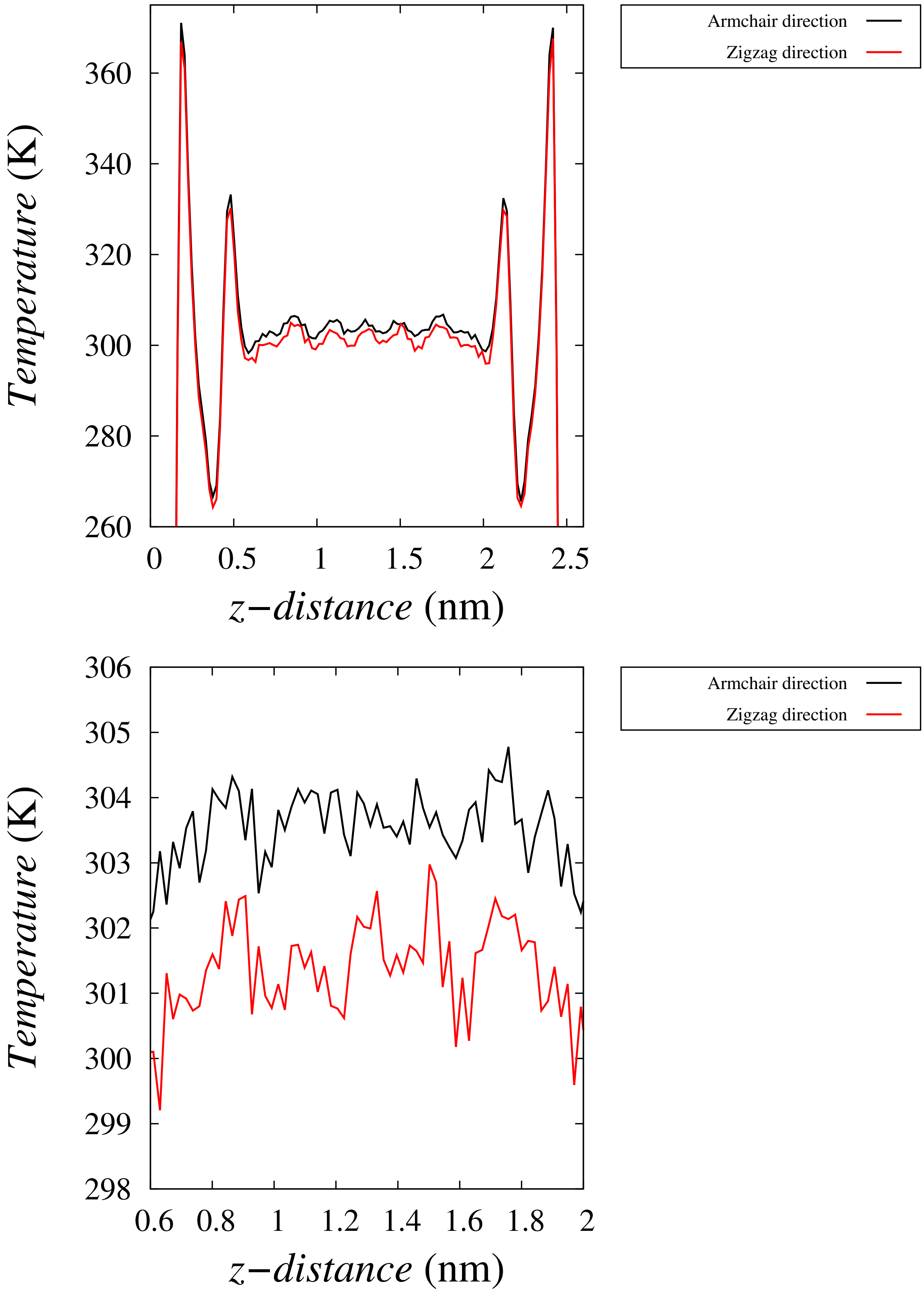

Figure 4 A) Temperature profiles for the $8 \cdot 10^{11}$ m/s^2 applied external force for the 2.8 nm armchair and zigzag cases. The thermostat was coupled to the graphene atoms B) Zoom to the bulk zone of the same cases.

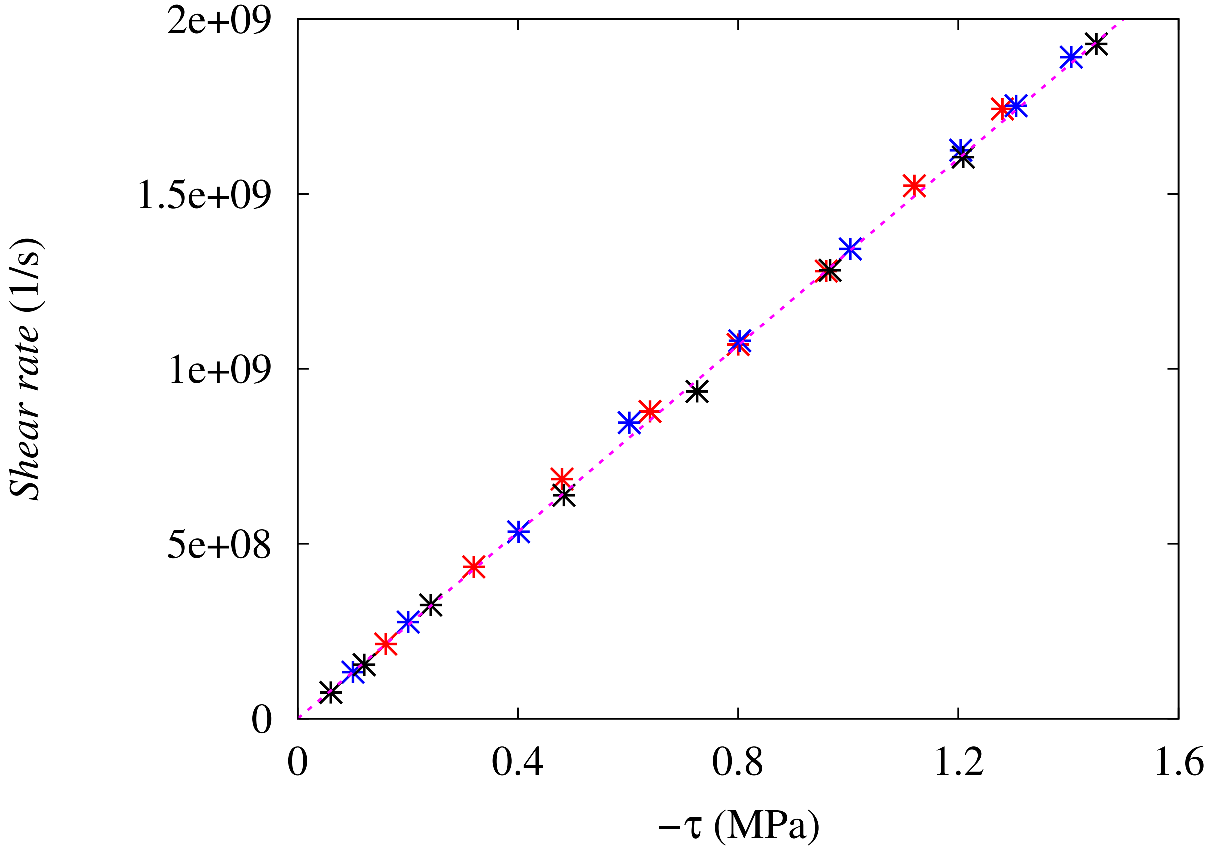

Figure 5 Shear rate as a function of the shear stress